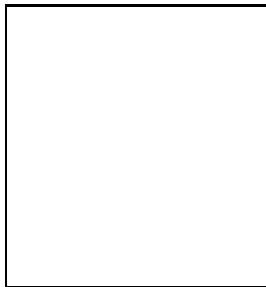


Gravitational Effects on Particle Dark Matter and Indirect Detection

Günter Sigl, Gianfranco Bertone

GReCO, Institut d'Astrophysique de Paris, C.N.R.S., 98 bis boulevard Arago, F-75014 Paris, France



The annihilation signal of particle dark matter can be strongly enhanced in over-dense regions such as close to the Galactic centre. We summarize some of our recent results on fluxes of γ -rays, neutrinos and radio waves under different assumptions for the largely uncertain dark matter profile which close to the Galactic centre is strongly influenced by the super-massive black hole. We apply this to two particle dark matter scenarios, namely the case of neutralinos in supersymmetric scenarios and the lowest Kaluza-Klein excitation of the hyper-charge gauge boson in scenarios where the Standard Model fields propagate in one microscopic extra dimension.

1 Introduction

Over the last thirty years, independent pieces of evidence have accumulated in favor of the existence of *Dark Matter* (DM), indicating that most of the matter of the universe is non baryonic and of unknown nature. Particle physicists have come up with various DM candidates. The most promising and most extensively studied is the so-called *neutralino*, the Lightest Supersymmetric Particle (LSP) which arises in supersymmetric models and is stable in models with conserved R-parity¹.

Although theoretically well motivated, *neutralinos* are not the only viable DM candidates. For instance, models with compact extra dimensions possess plenty of new states, Kaluza-Klein (KK) particles. In models with *Universal Extra Dimensions*², in which all Standard Model fields propagate in extra dimensions, including fermions, the Lightest Kaluza-Klein Particle (LKP) can be stable and was recently shown to be a viable DM candidate³. Precision electroweak measurements put a lower limit of $M \gtrsim 300 \text{ GeV}$ on the mass of the LKP² in the case of one universal extra dimension.

Indirect signatures of DM are typically proportional to the line of sight integral of the squared density. Unfortunately, there is still no consensus about the shape of dark matter halos. High-resolution N-body simulations suggest the existence of “cusps”, with the inner part of the halo

Table 1: Parameters of some widely used profile models, namely the Kravtsov et al. (Kra,⁷), Navarro, Frenk and White (NFW,⁸), Moore et al. (Moore,⁹) and modified isothermal (Iso, e.g.¹⁰) profiles for the dark matter density in galaxies in Eq. (1).

	α	β	γ	R (kpc)
Kra	2.0	3.0	0.4	10.0
NFW	1.0	3.0	1.0	20
Moore	1.5	3.0	1.5	28.0
Iso	2.0	2.0	0	3.5

density following a power law $\propto r^{-\gamma}$ in the distance r to the Galactic centre (GC) with index γ possibly as high as 1.5, but it could also be $\simeq 1.0$ or shallower⁴. On the other hand observations of rotation curves of galaxies seem to suggest much shallower inner profiles⁵, but other groups claim the impossibility of constraining dark matter with such observations⁶).

The usual parametrisation for the dark matter halo density is

$$\rho(r) = \frac{\rho_0}{(r/R)^\gamma [1 + (r/R)^\alpha]^{(\beta-\gamma)/\alpha}} \quad (1)$$

In Tab. 1 we give the values of the respective parameters for some of the most widely used profile models.

Observations of the velocity dispersion of high proper motion stars suggest the existence of a super-massive black hole lying at the centre of our Galaxy, with a mass $\approx 2.6 \times 10^6 M_\odot$ ¹¹. It has been argued¹² that the process of adiabatic accretion of dark matter on this central super-massive black hole would in addition produce a “spike” in the dark matter density profile, leading to a power law index possibly as high as $\gamma \approx 2.4$. Although central spikes could be destroyed by astrophysical processes such as hierarchical mergers^{13,14}, these dynamical destruction processes are unlikely to have occurred for the Milky Way¹⁵. The existence of such spikes would produce a dramatic enhancement of the annihilation radiation from the GC, and would allow to put stringent constraints on dark matter particles properties and distributions^{12,16,17,15}. For an initially power-law type profile of index γ , as predicted by high resolution N-body simulations⁸, the corresponding dark matter profile after accretion is steepened to an index $\gamma_{sp} = (9 - 2\gamma)/(4 - \gamma)$ within 10^{-5} pc of the central black hole. For more details see¹²).

The observable annihilation flux of a secondary particle of type i (we focus on γ -rays and neutrinos) can be written as

$$\Phi_i(\psi, E) = \sigma v \frac{dN_i}{dE} \frac{1}{4\pi M^2} \int_{\text{line of sight}} ds \rho^2(r(s, \psi)) , \quad (2)$$

where the coordinate s runs along the line of sight, in a direction making an angle ψ respect to the direction of the GC. σv is the annihilation cross section, dN_i/dE is the spectrum of secondary particles per annihilation, and M is the DM particle mass.

The particle physics parameters σv and dN_i/dE depend on the model. For neutralino DM we use the DarkSUSY¹⁸ tool to select parameter values resulting in acceptable DM relic densities and being consistent with accelerator constraints. The LKP scenario has only one independent parameter, namely the LKP mass or, equivalently, the linear size of the extra dimension. The cross sections and branching ratios are then taken from³. The calculation of dN_i/dE in general involves three steps: Determination of the partial cross sections into lepton and quark final states, fragmentation of the quark final states into hadrons and decay of the hadrons into stable end products, namely nucleons, e^\pm , γ -rays, and neutrinos. For more details on the calculation of the secondary spectra dN_i/dE see¹⁹.

2 Gamma-Ray and Neutrino Fluxes

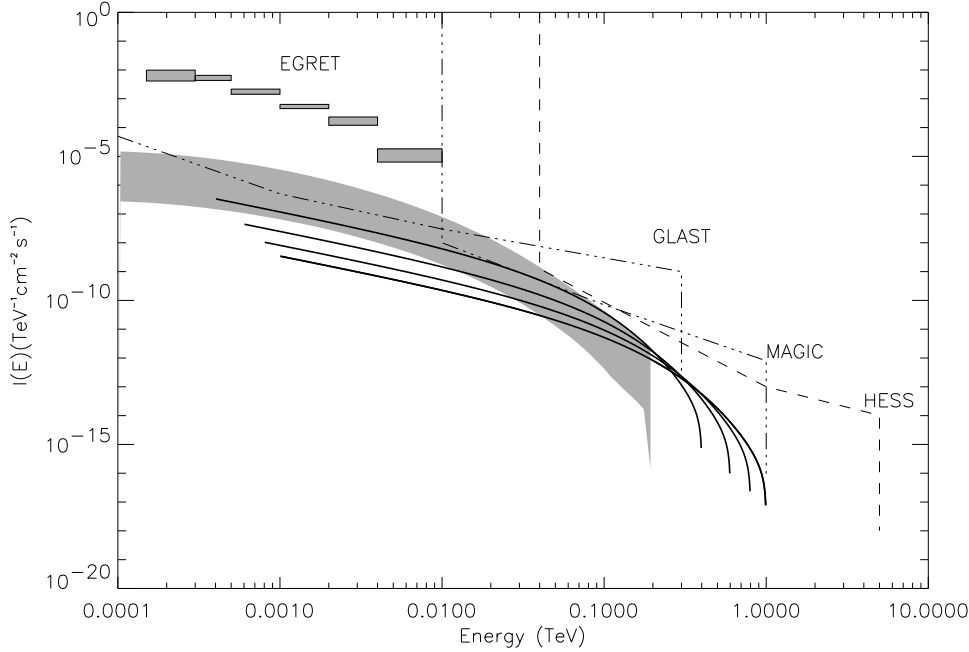


Figure 1: Expected γ -ray fluxes from the GC for the LKP scenario for (lines top to bottom) $M = 0.4, 0.6, 0.8$, and 1 TeV, assuming an NFW profile without accretion spike. The shaded area shows typical γ -ray fluxes predicted for neutralinos of mass $\simeq 200$ GeV. Also shown are EGRET data and expected sensitivities of the future GLAST, MAGIC and HESS experiments.

In Fig. 1 we show the γ -ray flux in a solid angle $\Delta\Omega = 10^{-3}$ in the direction of the GC predicted by Eq. (2) for some of the DM models discussed above, assuming a NFW profile without accretion spike. In the same figure we show for comparison observational data from EGRET²⁰, and expected sensitivities of the future experiments GLAST²¹, MAGIC²² and HESS²³.

As can be seen from Fig. 2, to explain the EGRET GC γ -ray flux would require DM slopes of $\gamma \simeq 1.5$ if no accretion spike is present. Presence of an accretion spike would instead require DM slopes $\gamma \simeq 0.1$ further out.

The neutrino fluxes are in general comparable to the γ -ray fluxes, but for a NFW profile without spike they are typically a factor $\sim 10^3$ below the sensitivity of experiments such as ANTARES and the Sun turns out to be a more easily detectable neutrino source in this case.

3 Synchrotron Radiation

Another interesting mean of indirect DM detection is the synchrotron radiation originated from the propagation of secondary e^\pm in the Galactic magnetic field.

The magnetic field is supposed to be at equipartition (for details see^{24,17}) in the inner part of the Galaxy and constant elsewhere. More specifically

$$B(r) = \max \left[324 \mu\text{G} \left(\frac{r}{\text{pc}} \right)^{-5/4}, 6 \mu\text{G} \right], \quad (3)$$

which means that the magnetic field is assumed to be in equipartition with the plasma out to a galactocentric distance $r_c = 0.23$ pc, and to be equal to a typical value observed throughout the Galaxy at larger distances.

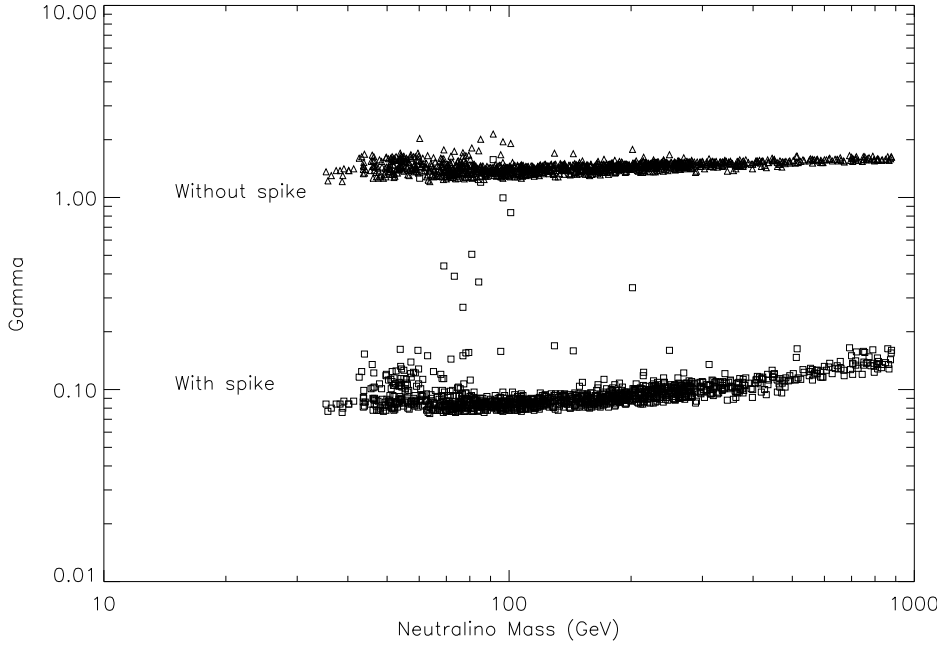


Figure 2: Required value of γ to reproduce the EGRET GC γ -ray flux for a typical set of supersymmetric DM models. Squares and triangles are for a halo model respectively with or without a central accretion spike.

Smaller magnetic fields away from the central region would imply a shift of the radio spectrum to lower energies and thus, in the range of frequencies we are interested in, a higher flux for a given frequency. This would also translate into stronger constraints on DM mass and annihilation cross section, thus Eq. (3) is likely to be conservative. Note that magnetic fields stronger than equipartition values are physically unlikely.

The energy loss of e^\pm is dominated by synchrotron radiation for which the loss time is much shorter than the diffusion length in magnetic fields of the order of Eq. (3)¹⁷. The synchrotron flux per solid angle at a given frequency ν (cf. Eq. (22) in¹⁷) can then be approximated by

$$L_\nu(\psi) \simeq \frac{1}{4\pi} \frac{9}{8} \left(\frac{1}{0.29\pi} \frac{m_e^3 c^5}{e} \right)^{1/2} \frac{\sigma v}{M^2} Y_e(M, \nu) \nu^{-1/2} \int_0^\infty ds \rho^2(r(s, \psi)) B^{-1/2}(r(s, \psi)), \quad (4)$$

where s is the coordinate running along the line of sight. $Y_e(M, \nu)$ is the average number of secondary electrons above the energy $E_m(\nu)$ at which synchrotron emission peaks at frequency ν for magnetic field strength B . For $r < r_c$,

$$E_m(\nu) = \left(\frac{4\pi}{3} \frac{m_e^3 c^5}{e} \frac{\nu}{B} \right)^{1/2} \simeq 0.3 \left(\frac{\nu}{400 \text{ MHz}} \right)^{1/2} \left(\frac{r}{\text{pc}} \right)^{5/8} \text{ GeV}, \quad (5)$$

which at the inner edge of the profile, corresponding to the Schwarzschild radius of the GC black hole, $r_s = 1.3 \times 10^{-6}$ pc, takes the value $E_m(400 \text{ MHz}) \simeq 2.2 \times 10^{-5}$ GeV. Since, therefore, $E_m(400 \text{ MHz}) \ll M$ always, basically all secondary e^\pm from DM annihilation are produced above this energy and contribute to the radio flux. Their number $Y_e(M) \simeq 5$ is again calculated from the specific particle physics model.

If an accretion spike is present, Eq. (4) is significantly modified by synchrotron self absorption whose effect we have estimated in¹⁷. In the absence of a spike self absorption is negligible. One can now compare the predicted radio flux with the one observed at 408 MHz in a cone of half-width 4 arcsec centered on the GC, which is $\lesssim 0.05 \text{ Jy}$ ²⁵. This yields the constraints on the

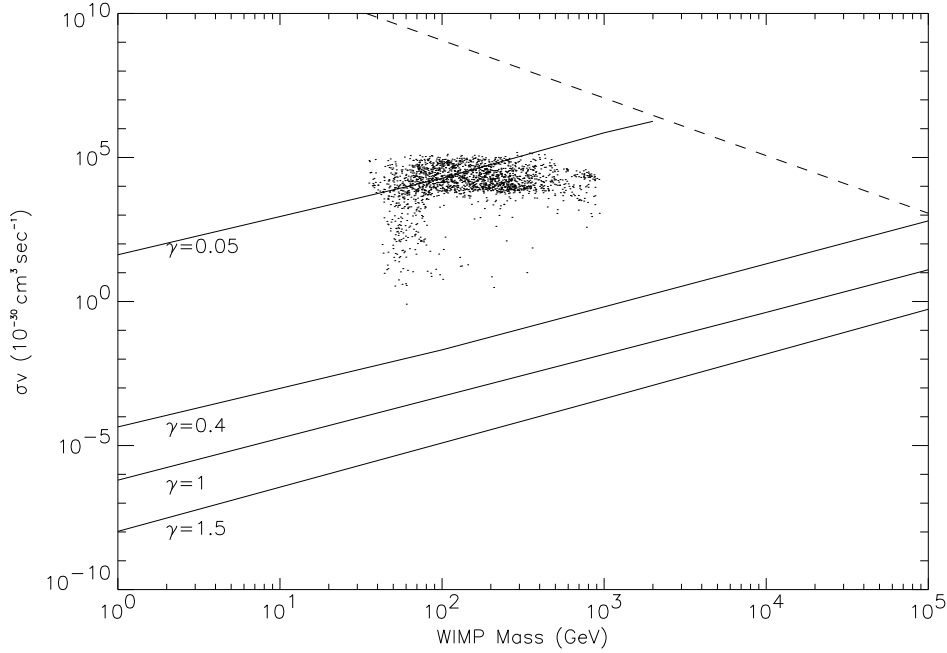


Figure 3: Exclusion plot based on the comparison between predicted and observed radio flux at 408 MHz from the inner 4 arcmin around the GC, assuming the presence of an accretion spike. The solid lines mark the upper limits on the annihilation cross section for various DM profiles γ outside the accretion spike. Dots represents a scan of SUSY neutralino DM and the dashed line represents the unitarity bound for s-channel annihilation, $\sigma v \lesssim M^{-2}$.

annihilation cross section shown in Fig. 3 if an accretion spike is present. In this case most neutralino models would be ruled out but for the most shallow DM profiles¹⁶ $\gamma \lesssim 0.05$.

In contrast, for a NFW profile without accretion spike one obtains the constraint

$$\sigma v \lesssim 1.5 \times 10^{-26} \left(\frac{M}{100 \text{ GeV}} \right)^2 \frac{5}{Y_e(M)} \text{ cm}^3 \text{ s}^{-1}. \quad (6)$$

This is at the high end of typical neutralino cross sections, see Fig. 3.

Constraints on the LKP scenario for various profiles without accretion spike are shown in Fig. 4. For a NFW profile, for example, the lower limit $M \gtrsim 300 \text{ GeV}$ results.

We also compared predicted and observed radio fluxes at high latitude. The strongest constraints result from the lowest frequencies at which free-free and synchrotron self-absorption are not yet important, i.e. around 10 MHz²⁶. Here, the observed background emission between 0° and 90° from the Galactic anti-centre is $\simeq 6 \times 10^6 \text{ Jy}$. Comparing with the predicted emission results in the limit

$$\sigma v \lesssim 10^{-24} \left(\frac{M}{100 \text{ GeV}} \right)^2 \frac{Y_e(1 \text{ TeV})}{Y_e(M)} \text{ cm}^3 \text{ s}^{-1}. \quad (7)$$

While this is considerably weaker than the constraints above, it is largely independent of the unknown GC dark matter profile.

4 Conclusions

We have discussed annihilation signals of dark matter from the Galactic centre and halo in the context of supersymmetric neutralino dark matter and Kaluza Klein states as dark matter in scenarios where Standard Model gauge boson fields propagate in one extra dimension. The largest uncertainties come from the unknown dark matter profile close to the Galactic centre.

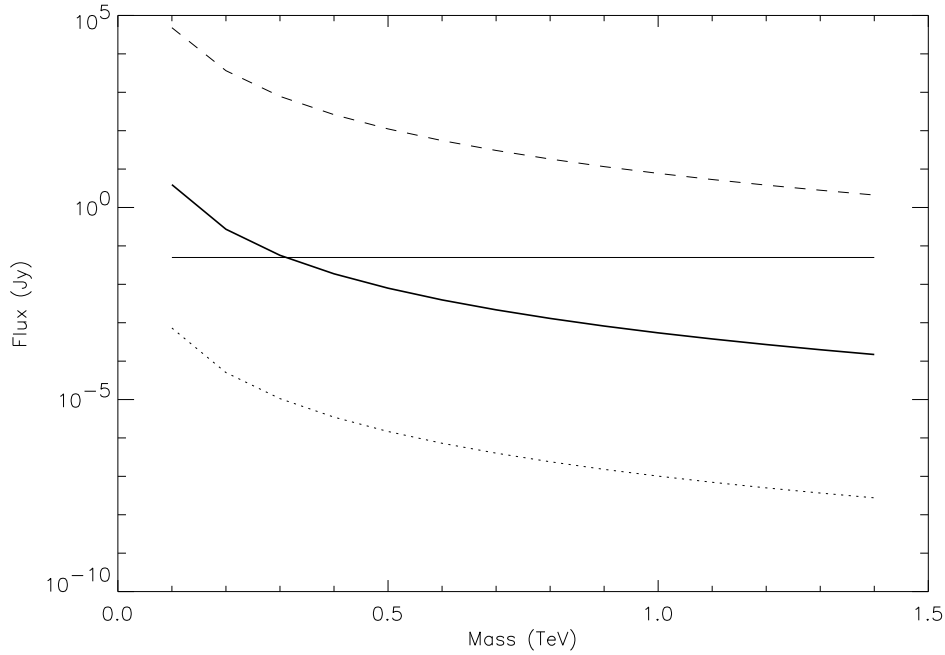


Figure 4: Radio flux from a 4 arcsec cone around the GC predicted in the LKP scenario as a function of the LKP mass for different density profiles. Bottom to top: Kravtsov et al. (dotted line), NFW (solid line) and Moore (dashed line) profiles.

Comparison of Fig. 2 and 4 shows that currently, assuming Eq. (3) for the magnetic field close to the Galactic centre, the synchrotron flux gives stronger constraints than the γ -ray flux. When instruments such as GLAST, MAGIC, and HESS will turn on, the γ -ray channel will provide constraining power comparable to the synchrotron channel, with the advantage that the γ -ray fluxes do not depend on the magnetic field uncertainties, although they may partly be absorbed. Our results on γ -rays are consistent with the findings in⁴ for a NFW profile without accretion spike which leads to fluxes marginally detectable with next generation γ -ray detectors. There it has also been shown that the clumpy structure of the dark matter in our Galaxy does not significantly strengthen the constraints. Finally, constraints based on the synchrotron emission may be enhanced by more systematically searching for directions in the sky where the ratio of predicted to observed radio flux is maximized.

Acknowledgments

This is based on work in collaboration with Joseph Silk and Geraldine Servant.

References

1. see, e.g., G.Jungman, M.Kamionkowski and K.Griest, *Phys. Rept.* **267**, 195 (1996).
2. T.Appelquist, H.C.Cheng and B.A.Dobrescu, *Phys. Rev. D* **64**, 035002 (2001).
3. G.Servant and T.M.Tait, *Nucl. Phys. B* **650**, 391 (2003).
4. F.Stoeckl et al., arXiv:astro-ph/0307026.
5. A.Salucci and P.Borriello, *Mon. Not. Roy. Astron. Soc.* **323**, 285 (2001).
6. F.C.van den Bosch and R.A.Swaters, arXiv:astro-ph/0006048.
7. A.V.Kravtsov, A.A.Klypin, J.S.Bullock, J.R.Primack, *Astrophys.J.* **502**, 48 (1998).
8. J.F.Navarro, C.S.Frenk and S.D.White, *Astrophys. J.* **462**, 563 (1996).

9. B.Moore, T.Quinn, F.Governato, J.Stadel and G.Lake, *Mon. Not. Roy. Astron. Soc.* **310**, 1147 (1999).
10. L.Bergstrom, P.Ullio and J.H.Buckley, *Astropart. Phys.* **9**, 137 (1998).
11. A.M.Ghez, B.L.Klein, M.Morris and E.E.Becklin, *Astrophys.J.* **509**, 678 (1998).
12. P.Gondolo and J.Silk, *Phys. Rev. Lett.* **83**, 1719 (1999).
13. P.Ullio, H.Zhao and M.Kamionkowski, *Phys. Rev. D* **64**, 043504 (2001).
14. D.Merritt, M.Milosavljevic, L.Verde and R.Jimenez, *Phys. Rev. Lett.* **88**, 191301 (2002).
15. G.Bertone, G.Sigl and J.Silk, *Mon. Not. Roy. Astron. Soc.* **337**, 98 (2002).
16. P.Gondolo, *Phys. Lett. B* **494**, 181 (2000).
17. G.Bertone, G.Sigl and J.Silk, *Mon. Not. Roy. Astron. Soc.* **326**, 799 (2001).
18. see <http://www.physto.se/~edsjo/darksusy/overview.html>.
19. G.Bertone, G.Servant and G.Sigl, arXiv:hep-ph/0211342.
20. H.A. Mayer-Haesselwander *et al.*, *A&A* 335, 161 (1998)
21. H.F.Sadrozinski, *Nucl. Instrum. Meth. A* **466**, 292 (2001).
22. D.Petry [the MAGIC Telescope Collaboration], *Astron. Astrophys. Suppl. Ser.* **138**, 601 (1999).
23. H.J.Völk, arXiv:astro-ph/0202421.
24. F.Melia, *Astrophys.J.* **387**, L25 (1992).
25. R.D.Davies, D.Walsh and R.S.Booth, *Mon. Not. Roy. Astron. Soc.* **177**, 319 (1976).
26. H.V.Cane, *Mon. Not. Roy. Astron. Soc.* **189**, 189 (1979).